Title page

Functional analysis of the UVR8 photoreceptor from the monocot *Zea mays*

Fernández María Belén[a], Lamattina Lorenzo[a], Cassia Raúl[a]*

[a] Instituto de Investigaciones Biológicas, Facultad de Ciencias Exactas y Naturales, Universidad Nacional de Mar del Plata- Consejo Nacional de Investigaciones científicas y Técnicas, CC1245 (7600). Mar del Plata, Argentina.

*Corresponding author: raul.cassia@gmail.com, 54-223-4753030 Int 16

Acknowledgements

We acknowledge Dr. Rius from CEFOBI institute for technical support with maize samples.

Funding

This study was funded by the Agencia Nacional de Promoción de Ciencia y Técnica (ANPCYT) grant number 3589, and Universidad Nacional de Mar del Plata grant number EXA 818/17. LL and RC are permanent researcher of CONICET Argentina. MBF has post-doctoral fellowship of Comisión de Investigaciones Científicas (CIC).

Conflict of Interest

The authors declare that they have no conflict of interest.

Abstract

Low UV-B fluence is a signaling stimulus that regulates various physiological processes and induces photomorphogenic responses in plants. The specific UV-B receptor UVR8 is a key component in these processes. Although UVR8 sequence is conserved, few homologs have been cloned and reported to be functional. Here we show the cloning and functional analysis of *Zea mays* UVR8 (*Zm*UVR8). *Zm*UVR8 presents 73% of identity with *At*UVR8, maintaining the key tryptophan responsible of UV-B perception. *Zm*UVR8 also contains the VP domain, involved in the interaction with the proteins CONSTITUTIVELY PHOTOMORPHOGENIC 1 (COP1) and REPRESSOR OF UV-B PHOTOMOPHOGENESIS 1 (RUP1). Whereas *UVR8* was expressed in non-irradiated *Arabidopsis* and maize leaves, after 2h of UV-B irradiation, its expression was reduced. The expression of chalcone synthase (*CHS*), involved in flavonoid biosynthesis and regulated by UVR8, was increased in irradiated *Arabidopsis* and maize leaves. *Arabidopsis uvr8-1* null mutant was complemented with *Zm*UVR8 driven by the CaMV-35S promoter and fused to eGFP. *Zm*UVR8-eGFP fusion was mainly localized in nuclei of transgenic lines, irrespective of UV-B treatments. UV-B suppressed hypocotyl elongation in WT *Arabidopsis* plants, whereas in *uvr8-1* hypocotyl growth was observed. However, hypocotyl elongation was reduced in UV-B irradiated transgenic lines complemented with *Zm*UVR8. Moreover, *CHS* and transcription factor *HY5* (ELONGATED HYPOCOTYL 5) expression were also restored in these plants. These results confirm that *Zm*UVR8 is similar enough to *At*UVR8 to restore UV-B perception and signaling in *Arabidopsis* mutant *uvr8-1*, thus being a functional UV-B photoreceptor.

Keywords

UVR8; UV-B; maize; monocot; *Arabidopsis*.

1. Introduction

Ultraviolet-B (UV-B) radiation is the region between 280 and 315 nm of the total Sun´s electromagnetic spectrum. Ultraviolet irradiances reaching the surface of the Archean Earth were higher than the current ones because of the absence of a significant ozone atmosphere (Cnossen et al. 2007). UV-B is higher in terrestrial environments compared to the water column (Rozema et al. 2002). High UV-B doses damages DNA, proteins, lipids, cell membranes, photosynthetic machinery and induces the production of reactive oxygen species (ROS). This affects plant cell integrity and viability, leading to growth retardation and to a decrease in crop yield and quality (Brosché and Strid 2003; Frohnmeyer and Staiger 2003; Jordan 1996). Consequently, plants evolved mechanisms to avoid UV-B damage during the colonization of exposed habitats (Tilbrook et al. 2013). Ancient photosynthetic organisms like cyanobacteria and various eukaryotic algae, use mycosporine-like amino acids (MAAs) as protective compounds against UV-B (Llewellyn and Airs 2010; Rastogi and Incharoensakdi 2013; Rozema et al. 2002). Land plants co-evolved with environmental UV-B levels, and the complexity of UV-B absorbing molecules increased accordingly from algae to higher plants (Rozema et al. 2002). The protein UV RESISTANCE LOCUS (UVR8) was identified as the specific UV-B receptor in plants (Brown et al. 2005). UVR8 signaling significantly contributes to UV-B acclimation responses and the establishment of UV-B tolerance. UVR8 regulates metabolic and developmental processes and induces physiological and photomorphogenic responses. The usually UVR8-mediated UV-B responses are the inhibition of hypocotyl growth and the accumulation of flavonols and anthocyanins. However, nowadays it is suggested that additional physiological responses are modulated by UVR8: phototropism, thermomorphogenesis, circadian clock, auxin signaling, defense, salt stress tolerance, shade avoidance, chloroplast development, stomatal opening, leaf development and downward leaf curling (for a review see (Yin 2017)).

Chlorophytes are the earliest organisms with an UV-B photoreceptor, *Chlamydomonas reinhardtii* being the first organism to own a functional UVR8 (Fernandez et al. 2016; Han et al. 2019). Since its discovery in 2005 (Brown et al. 2005), cumulative evidence allows us to consider a landscape of UVR8 interactions. In the absence of UV-B, the UVR8 homodimer is mainly located in the cytoplasm. In the nucleus, the E3 Ubiquitin ligase COP1 (CONSTITUTIVELY PHOTOMORPHOGENIC 1) represses the activity of the

transcription factor HY5 (ELONGATED HYPOCOTYL 5) (Favory et al. 2009). The transcription factor WRKY36 (WRKY DNA-BINDING PROTEIN 36) represses HY5 (Yang et al. 2018), and BES1 (BRI1-EMS-SUPPRESSOR1) and BIM1 (BES1-INTERACTING MYC-LIKE 1) induce BR-responsive gene expressions (Liang et al. 2018).

Following UV-B irradiation, UVR8 rapidly monomerizes and interacts in the nucleus with COP1 and WRKY36. This complex avoids the degradation of HY5, and induces the *HY5* expression. In turn, it triggers the UV-B regulated gene expression, leading to plant acclimation and stress tolerance (Heijde and Ulm 2012). Two of the HY5 upregulated genes are the Repressor of UV-B photomorphogenesis 1 and 2 (RUP1 and RUP2). Interaction of UVR8 with these proteins facilitates UVR8 dimerization, and subsequent inactivation (Heijde and Ulm 2012; Ulm and Jenkins 2015). UVR8 also interacts with BES1 and BIM1, inhibiting the brassinosteroid responsive genes, and reducing the hypocotyl elongation (Sun and Zhu 2018). Recently, it has been shown that the UVR8-COP1 complex participates in the PHYTCHROME INTERACTING FACTOR (PIF) 4 y 5 degradation, causing the UV-B-induced hypocotyl shortening (Sharma et al. 2019; Tavridou et al. 2019).

UVR8 is the first photoreceptor described that perceives UV-B through tryptophan residues instead of a prosthetic chromophore (O'Hara and Jenkins 2012; Ulm and Jenkins 2015).Two *Arabidopsis* UVR8 (*At*UVR8) high- resolution crystal structures have been determined using different crystallization conditions. However, they proved to be nearly identical in tertiary and quaternary structure (Christie et al. 2012; Wu et al. 2012; Yang et al. 2016; Zeng et al. 2015). *At*UVR8 contains a core domain that forms a seven-bladed β-propeller and a flexible C-terminal region of approximately 60 amino acids that contains a C27 region. Both the β-propeller domain and the C-terminal C27 domain of UVR8 are necessary and sufficient for interacting with COP1. Moreover, UVR8 interacts also with WRKY36 by its C- terminal (aminoacids 397 to 440) (Yang et al. 2018). *At*UVR8 has fourteen tryptophan residues, seven of which are exposed to the dimer interface. It also contains three conserved pentapeptide repeats with the motif “GWRHT” in blades 5, 6, and 7. This motif generates a closely clustered triad of tryptophans (W233, W285 and W337) which are the most important for UV-B photoreception (Christie et al. 2012; Wu et al. 2012; Zeng et al. 2015). Structural and mutagenesis studies show a primary role for W285 and W233in UV-B perception, whereas

W337 is not essential in this process (Christie et al. 2012; Sun and Zhu 2018; Wu et al. 2012). The motif "GWRHT" from blade 6 contains W285 and is conserved in all UVR8 homologs analyzed (Fernandez et al. 2016; Han et al. 2019).

Zea mays also known as corn, is a cereal grain of agronomic importance, and has been used as a model organism in basic and applied research for nearly a century (Strable and Scanlon 2009). Previous work shows that increased UV-B radiation produces a significant reduction in dry matter accumulation and, consequently, affects yield. Moreover, an increase in flavonoid accumulation, a decrease in chlorophyll content in leaves and a reduction in protein level, sugar and starch of maize seeds have also been reported (Gao et al. 2004). In 2011, Casati et. al. described a transiently upregulation and subsequent downregulation of two UVR8- like genes upon UV-B exposure in maize leaves (Casati et al. 2011a; Casati et al. 2011b). However, these genes have little homology to *At*UVR8 as they were identified by homology to rice genome.

Although UVR8 is conserved, and sequences for this gene are found in all the *Viridiplantae* (Fernandez et al. 2016; Han et al. 2019), a few UVR8 homologs have been cloned and reported to be functional from green algae, moss and dicots. Up to now, there is no evidence of UVR8 photoreceptor from monocotyledon plants with confirmed functionality. Here, we report the molecular cloning, sequence and functional complementation of *Zm*UVR8, the UV-B receptor of *Zea Mays*.

1. Material and Methods

1.1. Plants material and growth conditions

Seeds of wild- type (WT) *Arabidopsis thaliana* ecotype *Landsberg erecta* (Ler) and the *uvr8-1* null mutant (Cloix et al. 2012) were kindly provided by Dr. Gareth Jenkins (University of Glasgow, Scotland). Seeds were surface sterilized in 30% (v/v) commercial bleach for one minute, rinsed with distilled sterile water and stratified for 72h at 4°C in darkness. Germinated seedlings were grown on agar plates containing half- strength Murashige and Skoog (MS) salts or in soil/ perlite/ vermiculite (3:1:1, v/v) under white light (160 $\mu mol.m^{-2} s^{-1}$, fluorescent tubes) and long- day regime (light/dark: 16/8h) at 25°C in an environment controlled chamber.

139 Maize (*Zea mays* B73 inbreed line) seeds were kindly provided by Dr. Sofía Eugenia Olmos
140 (INTA Pergamino, Argentina). Seeds were surface sterilized with 30% (v/v) commercial
141 bleach for 20 minutes and rinsed in distilled water. Subsequently, seeds were germinated on
142 water saturated filter paper in Petri dishes for 4-5 days and maintained at 25°C. Germinated
143 seedlings were grown on soil/ vermiculite (3:1, v/v) under a long- day regime (light/dark:
144 16/8 h) at 25°C in an environment controlled chamber with white light at 160 $\mu mol.m^{-2}\ s^{-1}$.
145 The topmost leaf from V6 developmental stage (when sixth leaf are visible in the leaf whorl)
146 plants was used for experiments.

147 **1.2. Generation of transgenic *Arabidopsis* plants expressing *Zm*UVR8**

148 The full length coding sequence from *Zm*UVR8 was amplified by PCR using the maize full-
149 length EST ZM_BFb0066P22.r (Arizona Genomics Institute) as template, and the specific
150 primers *Zm*UVR8-Fw and *Zm*UVR8Rv (Table 1). The amplified cDNA was cloned into the
151 entry pENTR/D-TOPO vector and confirmed sequence, orientation and reading frame by
152 DNA sequencing (Macrogen). The obtained entry clone was recombined with the Gateway
153 pH7FWG2 binary destination vector for 35S-driven expression in plants, with C-terminal
154 fusion to eGFP (35S::*Zm*UVR8- eGFP) (Karimi et al. 2002). This vector was introduced in
155 the *Agrobacterium* strain GV3101 by electroporation (Koncz and Schell 1986).
156 Transformation into *uvr8-1* mutant *Arabidopsis* was performed by floral dip (Clough and
157 Bent 1998). Transformants were selected based on its ability to survive on half- strength
158 Murashige and Skoog medium supplemented with 1% sucrose containing 15 mg L^{-1}
159 hygromycin. Resistant seedlings were then transferred to soil and grown under conditions
160 described above.
161 The transgenic lines generated were shown to have the transgene integrated at a single genetic
162 locus through segregation analysis. Homozygous T3 (#6.5) and T4 (#5.1.7) independent lines
163 were obtained by self-crossing and were used for the experiments. The level of transgene
164 expression in each line was examined by qRT-PCR and immunoblot.

165 **1.3. UV-B Treatments**

166 For experiments involving UV-B light treatments, *Arabidopsis* seedlings were exposed 2h to
167 white light (100 $\mu molm^{-2}s^{-1}$, fluorescent tubes) supplemented with 3.47 $\mu mol\ m^{-2}s^{-1}$
168 narrowband UV-B (Philips TL 100W/01) in a controlled environment chamber. The UV-B

169 dose used is similar to the radiation measured from sunlight at midday in Mar del Plata
170 summer (38.0055° S, 57.5426° W).
171 Maize plants were exposed for 0, 2 and 4h to white light (100 μmol.$m^{-2}s^{-1}$, fluorescent tubes)
172 supplemented with 8.81 μmol $m^{-2}s^{-1}$ narrowband UV-B (Philips TL 100W/01) in a controlled
173 environment chamber.
174 The spectral irradiance was determined with an Ultraviolet- B photo-radiometer (Delta ohm
175 HD2102.1).

176 **2.4. Expression analysis**

177 For gene expression quantification, plant materials were harvested, frozen in liquid nitrogen and
178 grounded under RNase-free conditions. Total RNA was extracted using TRIzol method, and treated
179 with DNase I (Invitrogen) at 37°C for 30 min, following the manufacturer‘s instructions. Then, the
180 RNA was reverse-transcribed using the M-MLV reverse transcriptase (Thermo) following the
181 manufacturer’s instructions. cDNA obtained was used for quantitative RT-PCR using Power SYBR
182 Green PCR mix and a StepOne machine (Applied Biosystems). Primers used are listed in Table 1. PCR
183 conditions were: 10 min at 95 °C, 40 cycles of 15 s at 95 °C and 1 min at 60°C. After amplification, a
184 melting curve analysis was performed, which resulted in a single product specific melting curve.
185 Negative controls for cDNA synthesis and qRT-PCR reactions were included in all cases. LineReg
186 program was employed for the analysis of gene expression (Ruijter et al. 2009). The transcript
187 relative quantifications were determined from the ratio between the starting concentration value
188 of analyzed mRNA and the reference genes actin2 for *Arabidopsis* samples or thioredoxin- like (Thr)
189 for maize as previously reported (Casati and Walbot 2004). The data shown are representative of at
190 least three independent experiments.

191 **Table 1** List of primers used in this work.

Primers			Sequence (5´→ 3´)	Amplicon length (pb)	Usage
Cloning	*Zm* UVR8	Fw	CACCGCTCCCGTTCCTCGCGGTGGTCAC	1341	Amplification of full length *Zm* UVR8
		Rv	TGATGACTGCACGCGCATCCTCTTCACGTCGT		
qRT-PCR	*Zm* UVR8	Fw	GTTTGGGTGTCGCCGTC	123	Amplification of *Zm* UVR8
		Rv	CCTCTTCACGTCGTTCTCC		
	Zm Thr	Fw	GGACCAGAAGATTGCAGAAG	104	Thioredoxin- like, maize reference gene
		Rv	CAGCATAGACAGGAGCAATG		
	Zm CHS	Fw	AGCTCGATCGCTAGCTCCTC	196	Maize chalcone synthase
		Rv	TCCCCCTCGATCTTTCTCCC		
	At UVR8	Fw	CCAGATTTCGGGAGGTTGG	102	Amplification of *At* UVR8
		Rv	TTATTGCCGACTCCTACTTGTCC		
	At Actin2	Fw	GTATTGTGCTGGATTCTGGTG	119	*Arabidopsis* reference gene
		Rv	GAGGTAATCAGTAAGGTCACG		
	At CHS	Fw	CAGACAGGACATCGTGGTGGT	102	*Arabidopsis* chalcone synthase
		Rv	ACATGAGTGATCTTTGACTTGG		

For protein assays, leaves were harvested into liquid nitrogen and proteins extracted in 100mM buffer KPO4 (pH 7.4), 1mM EDTA and a cocktail of protease inhibitors. The homogenate was centrifuged for 10 min a 10000 x g at 4°C. Protein concentration was determined by a Bradford assay. Thirty micrograms of total protein were loaded for *Zm*UVR8 protein expression and separated by 12% denaturing SDS-PAGE. Immunoblots were incubated with anti-GFP antiserum as primary antibody. After several washes, a secondary anti- mouse antibody conjugated to alkaline phosphatase and developed by NBT/BCIP staining. The membranes were stained with Ponceau S to reveal the Rubisco large subunit (rbcL) as loading control.

2.5. *Zm*UVR8- eGFP Subcellular Localization

Fifteen day old plants irradiated 1h with white light or white light supplemented with UV-B (3.47 $\mu mol.m^{-2}s^{-1}$), were vacuum infiltrated with 5 µg. mL^{-1} of Hoechst 33342 (Invitrogen Molecular Probes) in buffer PBS, 0.2% Triton-X100 for 4 min and maintained in shake at 50 rpm and darkness for 1h. Then, samples were washed 3 times with PBS. The subcellular localization of eGFP and Hoechst 33342 was visualized by a confocal laser scanning microscope (Nikon-C1siR Eclipse TiU) under oil (Biopack) with a ×40 objective. Images were taken using the Nikon EZ-C1 3.90 software. eGFP and Hoechst were excited using an argon laser at 488 nm and a laser at 408 nm, respectively. eGFP emission was collected

212 between 515 and 530 nm to avoid crosstalk with chloroplast autofluorescence. Hoechst
213 33342 fluorescence was collected at 440/50 nm. The same microscope settings for GFP and
214 Hoechst 33342 detection were used before and after UV-B illumination. Colocalization
215 analysis was performed on two independent transgenic lines. The data shown are
216 representative of at least three independent experiments.

217 **2.6. Hypocotyl length measurement**

218 Seedlings were grown for 5 days on agar plates of half strength Murashige and Skoog (MS)
219 salts containing 1% sucrose in white light or white light supplemented with 3.47 $\mu mol.m^{-2}$ s^{-}
220 ^{1} UV-B. Photographs were taken after treatments and hypocotyl lengths were measured using
221 the ImageJ software (http://rsb.info.nih.gov/ij). Three independent biological replicates were
222 performed for all experiments using al least 10 seedlings for each replicate ($n \geq 30$).

223 **2.7. Bioinformatic analysis**

224 Multiple sequence alignments were performed using MAFFT server
225 (http://mafft.cbrc.jp/alignment/server/) and edited with GeneDoc (Nicholas and Nicholas
226 1997).

227 **1. Results**

228 **3.1. An *At*UVR8 homolog with a conserved structure is found in maize.**

229 UVR8 sequences from green algae (*C. reinhardtii* (Tilbrook et al. 2016)), moss *(P. patens*
230 (Soriano et al. 2018)), liverworth (*M. polymorpha* (Soriano et al. 2018)) and dicots (*S.*
231 *lycopersicum* (Li et al. 2018a)*, M. domestica* (Zhao et al. 2016)*, V. vinifera* (Liu et al. 2014)*,*
232 *B. platyphylla* (Li et al. 2018b) and *P. euphratica* (Mao et al. 2015)) have been cloned,
233 characterized, and shown to restore the loss-of-function of the UVR8 null mutant *uvr8-1*
234 (Kliebenstein et al. 2002).
235 However, no monocot functional UVR8 protein has been reported so far. To this end, the
236 *Arabidopsis* protein sequence (AAD43920.1) was used as bait in a PSI-BLASTp for
237 searching the UVR8 homolog in maize, using the NCBI (www.ncbi.nlm.nih.gov/) and
238 Phytozome databases (www.phytozome.jgi.doe.gov/pz/portal.html). One sequence was
239 found (GRMZM2G003565), herein named "*Zm*UVR8". Figure 1A shows the comparison
240 between *Zm*UVR8 and the other functional UVR8 homologs. *Zm*UVR8 has 443 amino acids

length, a calculated molecular mass of 47.15 kDa, and 73% of identity to *At*UVR8. Key tryptophan residues responsible of UV-B perception (W233, 285 and 337) are conserved in *Zm*UVR8, as well as the VP domain in the C27 region, involved in the interaction with COP1 and RUP (Figure 1A). Figure 1B shows that *Zm*UVR8 has the same domain profile than *At*UVR8, including the conserved tryptophans, the C27 domain and the seven repeated RCC1 domains.

A.

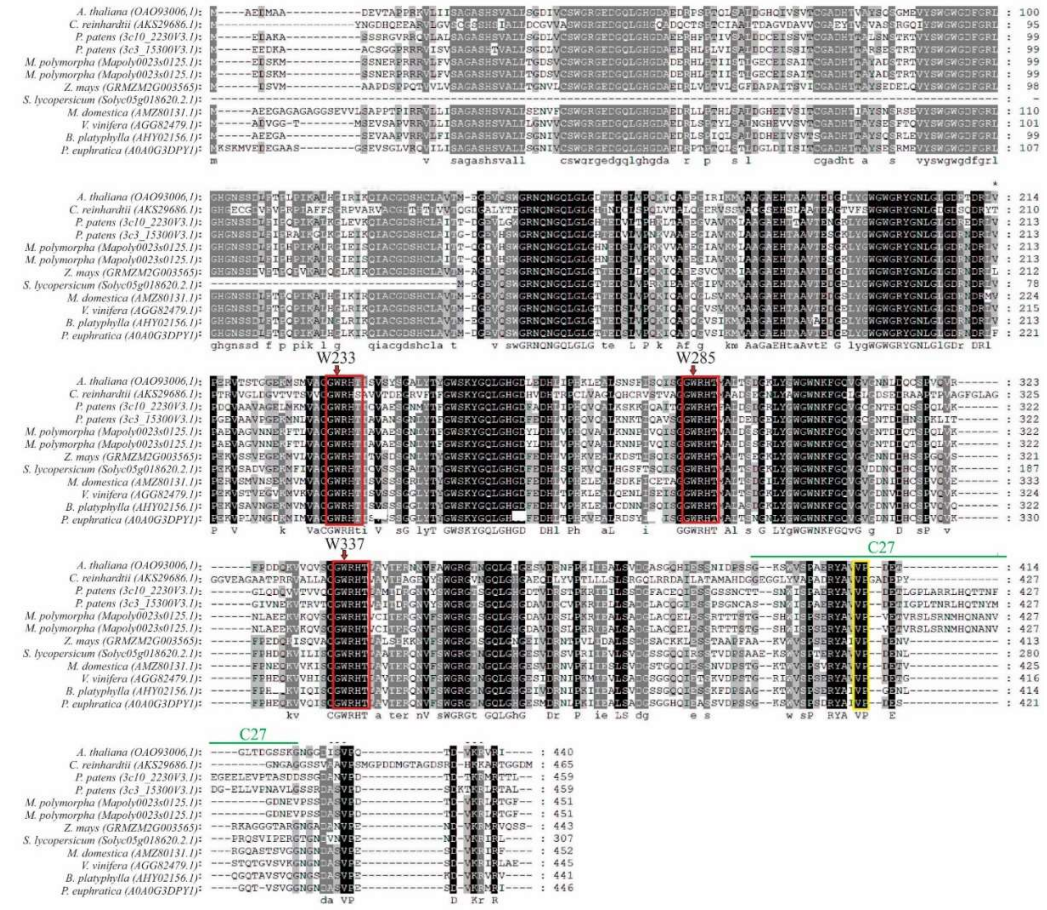

B.

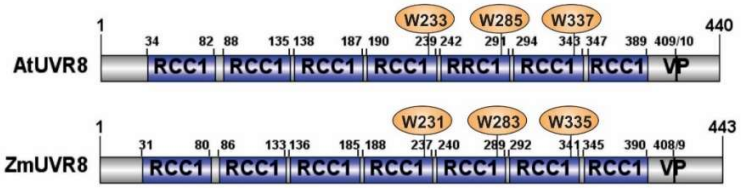

249 **Fig. 1 *Zm*UVR8 sequence and structural domains. A.** Multiple sequence alignment of *At*UVR8 homologs.
250 Sequences of proteins that restore the loss-of-function of the *uvr8-1* null mutant were aligned with MAFFT
251 (http://mafft.cbrc.jp/alignment/server/) and edited with GeneDoc (Nicholas and Nicholas 1997). Red boxes
252 indicate "GWRHT" motifs and the VP domain. The accession number of each sequence is given next to the
253 species name. Conserved residues common to all sequences are shadowed in black and less identity is shown
254 in gray scale. Capital letter indicates 100% of homology whereas lowercase indicates minor identity. The yellow
255 box shows the "VP" domain in the C27 domain, important for interaction with COP1 and RUP proteins. **B)**
256 Schematic representation of structural domains of *At*UVR8 and *Zm*UVR8 proteins. Analysis of amino-acid
257 sequences was performed at the National Center for Biotechnology Information (NCBI) database. RCC1
258 (pfam00415), Regulator of chromosome condensation (RCC1) repeat. Arrows indicate significant tryptophans
259 in UV-B perception (W233, 285 and 337). VP: Valine-Proline domain.

260

261 Blastp analysis in Table 2 shows that sequences with high percentage of identity with the
262 components of the *Arabidopsis* UVR8 signaling pathway were found in maize: COP1
263 (70%), HY5 (68%), HYH (48%), RUP1 (45%), RUP2 (46%), WRKY36 (35%), BES1
264 (50%) and BIM1 (41%). These results indicate that *Zm*UVR8 could be a functional UV-B
265 receptor, triggering a UVR8 signaling cascade in maize.

266

267 **Table 2. Identification of maize homologs to the *Arabidopsis* UVR8 signaling pathway.** Proteins involved
268 in UVR8 signaling cascade from *Arabidopsis* were used as bait in BLASTp analysis restricting the search to *Z.*
269 *mays* and the non- redundant protein sequences database from NCBI.
270

Arabidopsis protein	Bait ID	*Zea mays* identification	Identity (%)	E- value	Accession
COP1	NP_180854.1	Ubiquitin ligase protein COP1	70	0.0	AQK75277.1
Hy5	NP_001330553.1	Uncharacterized protein LOC100286123	68	9,00E-48	NP_001152483.1
HyH	NP_850605.1	Uncharacterized protein LOC100286123 isoform X1	48	3,00E-27	XP_008643871.1
RUP1	NP_200038.1	WD repeat-containing protein RUP2	45	5,00E-89	PWZ22039.1
RUP2	NP_568435.2	WD repeat-containing protein RUP2	46	2,00E-91	AQK67844.1
WRKY36	NP_564976.1	Probable WRKY transcription factor 31	35	4,00E-47	XP_008655458.1
BES1	NP_973863.1	BES1/BZR1 protein	50	7,00E-69	NP_001151195.2
BIM1	NP_001190259.1	Unknown	41	3,00E-49	ACN34591.1

271

272

273

274 **3.2. *Zm*UVR8 and *At*UVR8 expression are downregulated by UV-B irradiation.**

275 Previous studies show that *At*UVR8 is a ubiquitously expressed gene, allowing an immediate
276 reaction of plants to UV-B exposure (Favory et al. 2009; Rizzini et al. 2011). UVR8

277 expression was analyzed in *Arabidopsis* and maize plants irradiated with 3.47 and 8.81
278 µmol.m^{-2} s^{-1} of UV-B respectively. Figure 2 shows quantitative RT-PCR analysis of UVR8
279 expression in irradiated and non- irradiated leaves. After 2h of UV-B irradiation, UVR8
280 expression was reduced 3-fold in *Arabidopsis* and 6-fold in maize, respectively. However,
281 CHS expression was increased in both species after UV-B. These results indicate a similar
282 regulation of UVR8 and CHS expression under UV-B treatment both in *Arabidopsis* and
283 maize plants.

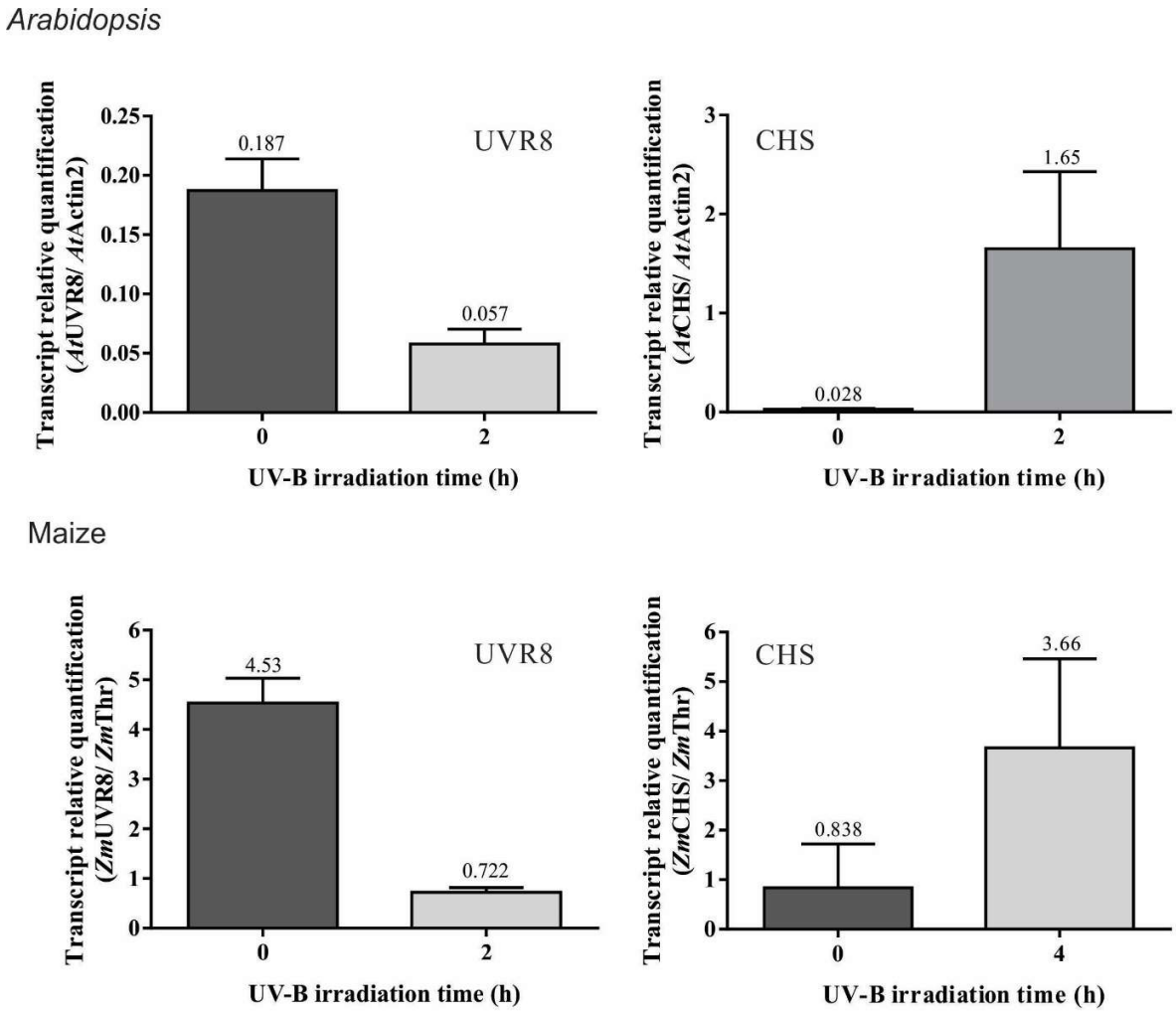

284
285
286 **Fig. 2 Expression of UVR8 and CHS in response to UV-B in *Arabidopsis* and maize plants.** UVR8 and
287 CHS transcript levels were analyzed by qRT-PCR. Three week–old *Arabidopsis* and maize plants were
288 irradiated during 2 and 4h with 3.47 and 8.81 µmol.m^{-2} s^{-1} of UV-B respectively. Non-irradiated plants were
289 used as control. Expression of Actin2 and thioredoxin- like (Thr) were used for *Arabidopsis* and maize

normalization respectively. Primers are listed in Table 1. Error bars indicate the standard deviation over three biological replicates (n=3).

Table 3 compares the expression of *ZmUVR8* with those of the other functional homologues. Whereas UV-B has no effect on *UVR8* expression in *M. polymorpha* and *V. vinifera* grapes, it upregulates transcript levels in different tissues from *M. domestica* and *B. platyphylla*. These findings, together with results shown in Figure 2, where *At*UVR8 and *Zm*UVR8 transcript levels were downregulated by this radiation, suggest the existence of different regulatory mechanisms for *UVR8* expression in different plant species and tissues.

Table 3. *UVR8* expression after UV-B stress in plant with confirmed UVR8 functional homologs.

Specie	Tissue	UVR8 expression in respopnse to UV-B	UV-B dose	Reference
Arabidopsis thaliana	Leaf	Downregulated after 2h of treatment	3.47 $\mu mol\ m^{-2}\ s^{-1}$	Figure 2
Chlamydomonas reinhardtii	nd			Tilbrook et. al., 2016
Physcomitrella patens	nd			Soriano et. al., 2018
Marchantia polymorpha	Plant	No significant effect of treatment after 3	3 $\mu mol\ m^{-2}\ s^{-1}$	Soriano et. al., 2018 Kondou et. al., 2019
Zea mays	Leaf	Downregulated after 2h of treatment	8.81 $\mu mol\ m^{-2}\ s^{-1}$	Figure 2
Solanum lycopersicum	nd			Li et. al., 2018
Malus domestica	Fruit skin	Upregulation after 6h of treatment	1.5 $\mu mol\ m^{-2}\ s^{-1}$	Zhao et. al, 2016
	Apple callus	Upregulation after 1h of treatment	1.5 $\mu mol\ m^{-2}\ s^{-1}$	
Vitis vinifera	Fruit	Not influenced by UV-B	Field radiation	Liu et. al., 2014
Betula platyphylla	Tissue culture seedling	Upregulation after 6h of treatment	1.5 $\mu mol\ m^{-2}\ s^{-1}$	Li et. al., 2018
Populus euphratica	nd			Mao et. al., 2015

Nd: not determined.

3.3 Transgenic *Zm*UVR8 expression in the *uvr8-1* null mutant

For insights into the *in vivo* role of *ZmUVR8*, we cloned the *ZmUVR8* cDNA into the pH7FWG2 plant expression vector driven by the CaMV-35S promoter and fused to eGFP (35S::*Zm*UVR8-eGFP). This construct was used to transform the *Arabidopsis uvr8-1* null mutant. After repeated selection on hygromycin and microscopy eGFP-screening, two independent T3 and T4 homozygous lines (#6.5 and #5.1.7 respectively) were obtained. *ZmUVR8* expression was determined by quantitative RT-PCR using specific primers that

did not amplify *At*UVR8 (Online resource S1). Figure 3A illustrates that both lines expressed *ZmUVR8* mRNA, line #6.5 reaching the highest level. Immunoblot with anti-GFP antibody in Figure 3B shows that *Zm*UVR8-eGFP was present in both transgenic lines.

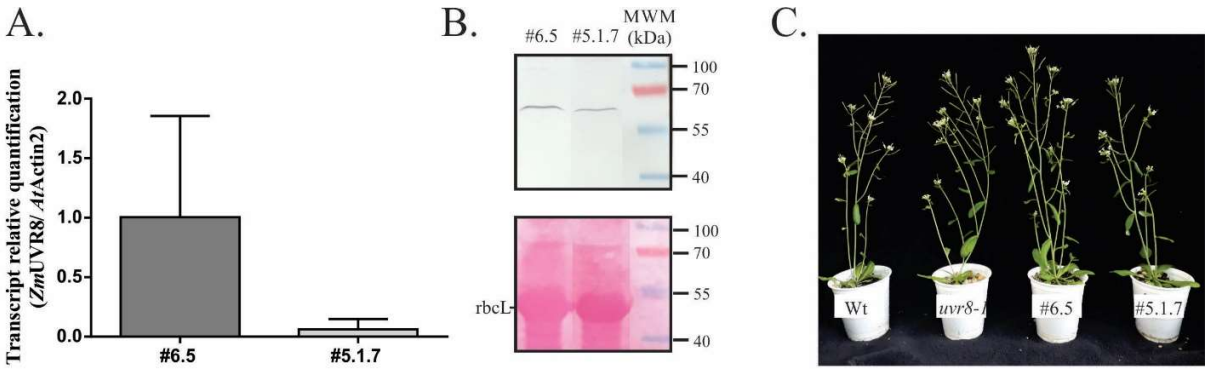

Fig. 3 35S::*Zm*UVR8-eGFP expression analysis in two *Arabidopsis* homozygous lines. A. Leaves from three-weeks-old transgenic *Arabidopsis* plants were used to analyze *Zm*UVR8 transgene transcript level by qRT-PCR. Expression of Actin2 was used for normalization. Primers are listed in Table 1. Error bars indicate the standard deviation over three biological replicates. **B.** Denaturating immunoblot from *Arabidopsis* transgenic lines #6.5 and #5.1.7 protein extracts (upper panel). Immunodetection was performed using anti-GFP antiserum. Stained Rubisco large subunit (rbcL) is shown as a loading control (lower panel). **C.** Thirty-days-old WT, *uvr8-1* mutant and #6.5 and #5.1.7 transgenic *Arabidopsis* lines.

Online resource S2 shows no positive GFP signal in WT lines, ensuring the specificity of *Zm*UVR8-eGFP detection. Figure 3C shows that *Zm*UVR8 has no detrimental effects on plant development, because no evident phenotypic differences were found among WT, *uvr8-1*, #6.5 and #5.1.7, after 30 days.

The sub-cellular localization of *Zm*UVR8-eGFP, was analyzed using a confocal laser scanning microscope. Hoechst 33342 staining was employed for nuclear staining. Figure 4

338 shows that *Zm*UVR8-eGFP fusion was mainly localized in nuclei of #6.5 and #5.1.7 lines,
339 irrespective of UV-B treatments.

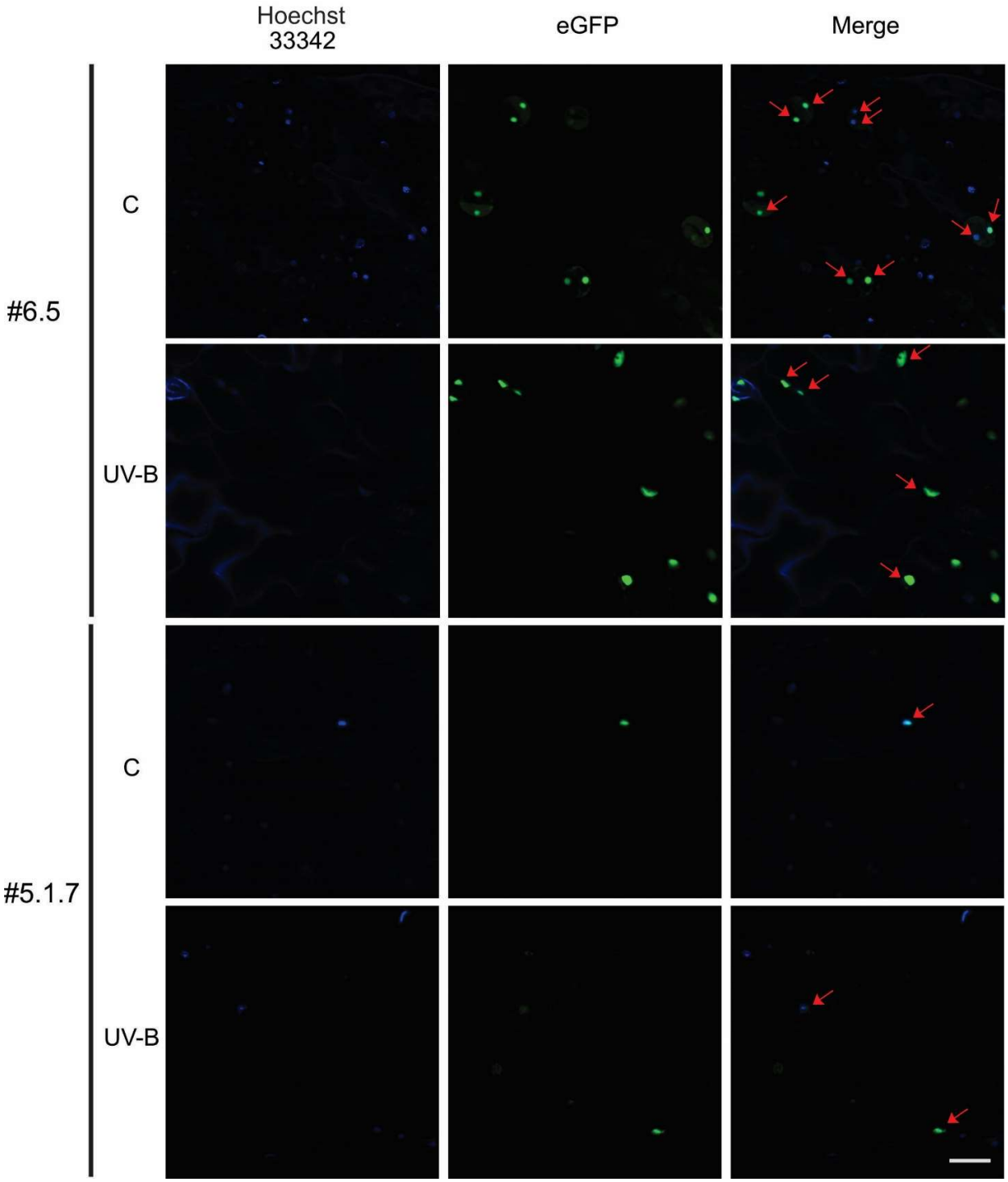

340

341

342 **Fig. 4 Subcellular localization of eGFP-*Zm*UVR8.** Cellular localization of *Zm*UVR8-eGFP fusions revealed
343 by confocal laser microscopy. Two-weeks-old *Arabidopsis* plants were irradiated with 100 $\mu molm^{-2}s^{-1}$ of white
344 light (C), or white light plus 3.47 $\mu mol.m^{-2}s^{-1}$ UV-B (UV-B) for 1 h. Hoechst 33342 was vacuum infiltrated to
345 specifically stain nuclei. eGFP and Hoechst were excited using a laser at 488 nm and 408 nm, respectively.
346 eGFP emission was collected between 515 and 530 nm to avoid crosstalk with chloroplast autofluorescence.
347 Hoechst 33342 fluorescence was collected at 440/50 nm. The same microscope settings for GFP and Hoechst
348 33342 detection were used before and after UV-B illumination. Bar: 25 µm. #6.5 and #5.1.7: transgenic
349 *Arabidopsis* lines expressing *Zm*UVR8-eGFP. Arrows indicate co-localization.

350

351

352 **3.4. *Zm*UVR8 complements the *Arabidopsis uvr8-1* null mutant**

353 The hypocotyl length inhibition is frequently used to analyze photoreceptors functionality in
354 *Arabidopsis*. UV-B suppresses hypocotyl growth in wild-type *Arabidopsis* plants, whereas
355 the *uvr8-1* mutant is impaired in this response (Favory et al. 2009). **E**xpression of WT
356 *At*UVR8 fused to GFP or yellow fluorescent protein (YFP) in *uvr8-1* plants, restores the WT
357 phenotype (Favory et al. 2009; Huang et al. 2014; O'Hara and Jenkins 2012). The recovering
358 of this morphogenic response was established as a parameter of functionality for several
359 UVR8 homologs (Kondou et al. 2019; Li et al. 2018a; Li et al. 2018b; Liu et al. 2014; Mao
360 et al. 2015; Soriano et al. 2018; Tilbrook et al. 2016; Zhao et al. 2016). Figure 5 shows no
361 differences among hypocotyl length of WT, *uvr8-1* and transgenic lines grown under white
362 light. Although #5.1.7 line grown under white light appears slightly shorter than *uvr8-1* and
363 #6.5 at the seedling stage, no differences were observed in 30-days-old plants (Fig. 3C).
364 Figure 5 B shows that, under UV-B irradiation, the reduction in hypocotyl length was of 54%
365 in WT plants. In contrast, the reduction in *uvr8-1* mutant was only of 31%. However,
366 hypocotyl elongation was reduced 50% in line #6.5 and 60% in line #5.1.7, similar to WT
367 plants (Fig. 5B). These results indicate that *Zm*UVR8 restore the *uvr8-1* null mutant
368 phenotype under UV-B radiation demonstrating that is a positive regulator in UV-B induced
369 photomorphogenesis.

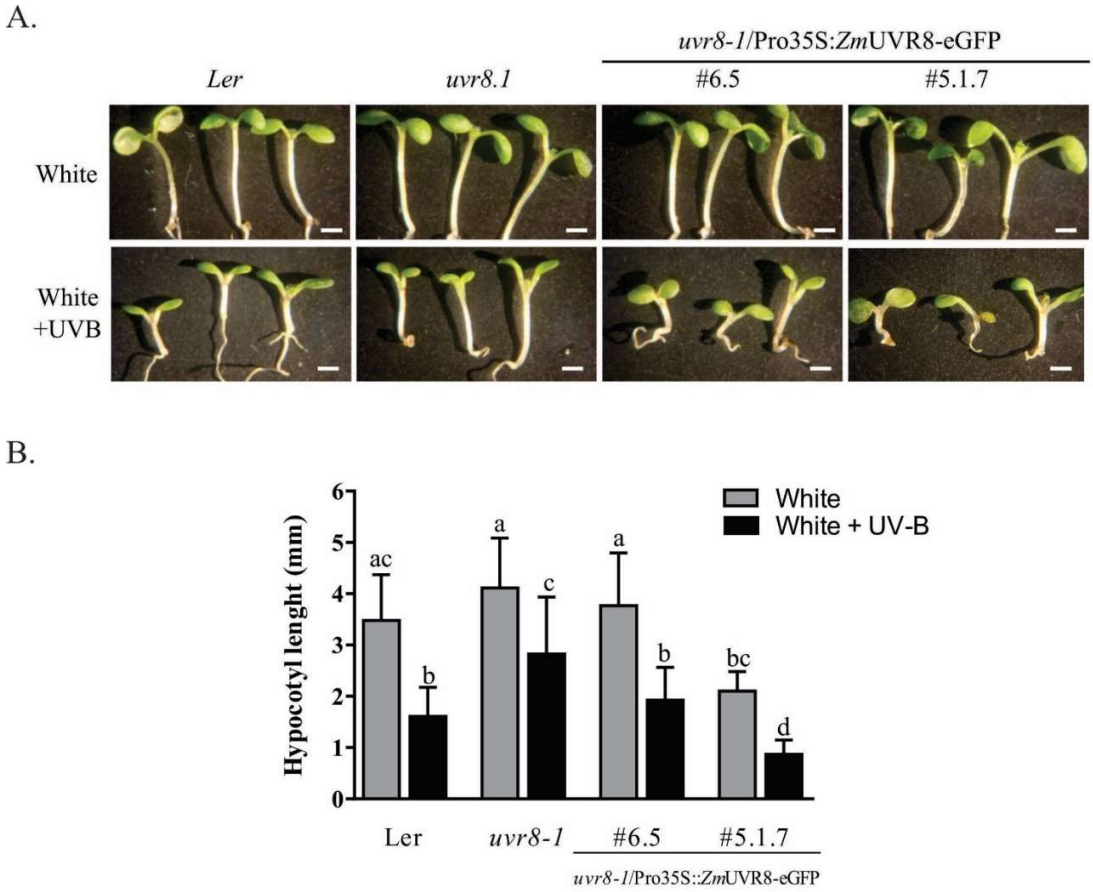

Fig. 5 Functional complementation assay of eGFP-*Zm*UVR8 expressed in *Arabidopsis uvr8-1* mutant. A. Phenotypes of the *Arabidopsis* WT, *uvr8-1*, and #6.5 and #5.1.7 lines grown under 100 µmolm^{-2}s^{-1} of white light, or white light plus 3.47 µmol.m^{-2} s^{-1} of UV-B. The scale bar represents 1mm. Photographs were taken after treatments. **B.** The hypocotyl lengths were measured using the ImageJ software (http://rsb.info.nih.gov/ij). Grey bars: white light, black bars: white light plus UV-B. Error bars indicate standard deviation. Different letters show significant differences between treatments (Kruskal- Wallis One-way ANOVA on ranks. Multiple comparisons: Dunn´s method, $p<0.05$). Three independent biological replicates were performed, n≥30.

*3.5.Zm*UVR8 promotes CHS and HY5 gene expression in *uvr8-1 Arabidopsis* mutant

In response to UV-B, plants increase the concentration of UV-B-absorbing phenolic compounds such as flavonoids. The enzyme chalcone synthase (CHS) catalyzes the first step of flavonoid biosynthesis and is regulated by the UVR8 signaling pathway (Jenkins 2014;

385 Yonekura-Sakakibara et al. 2019). UVR8-COP1-SPA complexes induce the expression of
386 the transcription factor HY5, which is a positive regulator of *CHS* expression (Jenkins 2014).
387 In order to determine if *Zm*UVR8 is able to induce *CHS* and *HY5* expression in response to
388 UV-B, three- weeks- old Ler, *uvr8-1* and #6.5 transgenic line plants were irradiated with
389 white light or white light supplemented with UV-B for 2 hours. *CHS* and *HY5* expression
390 was determined by quantitative RT-PCR. Figure 6 illustrates that, under white light
391 irradiation, *CHS* and *HY5* have low basal expression in all plants. After UV-B irradiation,
392 the expression of both genes was increased in WT plants, but the *uvr8-1* mutant was impaired
393 in this response. However, UV-B-irradiated #6.5 line increased *CHS* and *HY5* expression
394 (Fig. 6). These results, demonstrate that *Zm*UVR8 was able to trigger the UVR8 signaling in
395 response to UV-B.

396

397

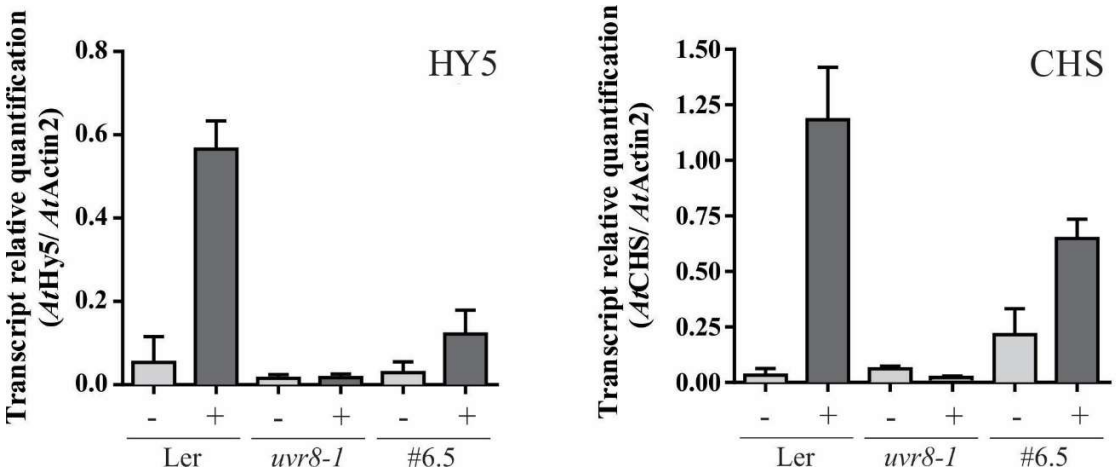

398

399

400 **Fig. 6 Expression levels of *CHS* and *HY5* in response to UV-B in WT, *uvr8-1* mutant and transgenic line**
401 **#6.5 under UV-B irradiation.** Three-weeks-old WT, *uvr8-1* and #6.5 transgenic line plants were exposed to
402 white light, or white light supplemented with 3.47 µmol.m^{-2} s^{-1} of UV-B for 2h. The expression of *CHS* and
403 *HY5* in leaves was determined by qRT-PCR. Expression of Actin2 was used for normalization. Error bars
404 indicate the standard deviation of at least two biological replicates.

405

406

407

408 **Discussion**

409 In this work we have cloned the maize *Zm*UVR8, the first functional UVR8 protein from
410 monocots homologue to the *Arabidopsis* UV-B receptor.

411 Two maize UV-B-responsive genes were previously reported as UVR8-like homologs by
412 comparison with rice genome (Casati et al. 2011a; Casati et al. 2011b). However, these genes
413 present less than 34% of identity with *At*UVR8, and tryptophans 233 and 285, involved in
414 UV-B perception, are not conserved (not shown). After the maize genome sequencing was
415 completed, we found *Zm*UVR8 and, by phylogenetic studies, we concluded that a unique
416 UVR8 sequence was present in maize (Fernandez et al. 2016). *Zm*UVR8 has a conserved
417 sequence and a modular structure, in concordance with several UVR8 homologs (Fernandez
418 et al. 2016). In addition, we found that maize proteins involved in UVR8 signaling have more
419 than 35% of identity with those from *Arabidopsis* (Table 2). Considering that 30% of identity
420 is enough to infer that two proteins are homologous (Pearson 2014), we suggest that the
421 UVR8 signaling cascade might be present in maize. Furthermore, phylogenetic studies
422 demonstrate that UVR8, SPAs and HY5 proteins are conserved from chlorophytes to
423 angiosperms (Fernandez et al. 2016; Han et al. 2019). Functional studies will be necessary
424 to confirm these hypotheses.

425 Although *UVR8* was reported as constitutive in *Arabidospsis*, we show herein that *UVR8*
426 transcript decreased both in *Arabidopsis* and maize leaves after 2 hours of UV-B radiation.
427 Likewise, *Betula platyphylla* UVR8 (*BpUVR8*) expression is induced by UV-B, and
428 decreases after 9h of continuous irradiation (Li et al. 2018b). On the other hand, *UVR8*
429 expression is increased by UV-B in the hypocotyls of radish sprouts (Wu et al. 2016).
430 Variations in *UVR8* expression were also reported in UV-B-treated fruit skin and apple callus
431 (Mao et al. 2015). Differences observed in *UVR8* expression in the literature could result
432 from the different UV-B intensities used in the experiments and tissues analyzed. *At*UVR8
433 is a stable protein (Heilmann and Jenkins 2013) and a huge amount of UVR8 may influence
434 the activity of COP1 and RUP as E3 ligases (Ren et al. 2019). It may be possible that after
435 UVR8 was translated, gene expression could be decreased to avoid UVR8 overaccumulation
436 in *Arabidopsis* and maize.

437 Little is known about the existence of different regulatory mechanisms for *UVR8* expression.
438 Wu et. al. (2016) proposed that UV-B enhances the production of H_2O_2, thus increasing the
439 level of NO to further magnify the *UVR8* expression. It was recently reported that *At*UVR8
440 expression may be modulated by blue light in UV-B-irradiated *Arabidopsis*. Cryptochrome
441 1 (Cry1) mutant *hy4* shows reduced *UVR8* expression in response to UV-B, suggesting a
442 linkage between cry1, *UVR8* and UV-B (Khudyakova et al. 2019). Besides, it has been
443 observed that *ZmUVR8* expression is increased by waterlogged in non-UV-B-irradiated
444 maize root (Rajhi et al. 2011).

445 We obtained two independent homozygous *Arabidopsis* lines (#6.5 and #5.1.7), where
446 *Zm*UVR8- eGFP complemented the *uvr8-1* null mutant both in hypocotyl elongation assay
447 and induction of UVR8-regulated genes. *Arabidopsis* GFP-UVR8 shows increased nuclear
448 localization following UV-B treatment of plants (Kaiserli and Jenkins 2007), but *Zm*UVR8-
449 eGFP was constitutively located in nuclei in #6.5 and #5.1.7 lines.

450 No obvious nuclear localization signal (NLS) is found in UVR8, and there is no consensus
451 about the mechanism of UVR8 translocation (Yin 2017). Yin et. al. (2016) reported that
452 UVR8 interaction with COP1 is necessary for UVR8 translocation to nucleus, as well as
453 for UVR8 signaling in response to UV-B (Yin et al. 2016). Moreover, it was demonstrated
454 that the presence of UVR8 in the nucleus is necessary but not sufficient for its function.
455 Kaiserli & Jenkins (Kaiserli and Jenkins 2007) fused a NLS to GFP-UVR8 and observed that
456 the constitutive nuclear localization of NLS-GFP-UVR8 is insufficient to promote *HY5*
457 expression in the absence of UV-B. Therefore, even though *Zm*UVR8 has nuclear
458 localization irrespective of UV-B treatment, this radiation is necessary for downstream
459 signaling as previously reported for *At*UVR8.

460 UV-B irradiation is not a mere stress signal but can also serve as an environmental stimulus
461 to direct growth and development. A well-established UV-B morphogenic effect is
462 the reduction of hypocotyl elongation (Kim et al. 1998). The hypocotyl growth of the *uvr8-*
463 *1* mutant seedlings, in stark contrast to wild-type seedlings, was not inhibited by UV-B
464 (Favory et al. 2009). The restoring of this morphogenic response was established as a
465 parameter of complementation by functional UVR8 homologs (Kondou et al. 2019; Li et al.

466 2018a; Li et al. 2018b; Liu et al. 2014; Mao et al. 2015; Soriano et al. 2018; Tilbrook et al.
467 2016; Zhao et al. 2016).

468 *Zm*UVR8 restored the impaired UV-B hypocotyl growth suppression, and the *CHS* and *HY5*
469 expression in *uvr8-1*, working as an effective component of the UVR8 pathway. These results
470 demonstrate that similar signaling responses to UV-B are present in monocots and dicots
471 plants. Consequently, a canonical UVR8 pathway could be present in monocotyledons.

472 **Conclusion**

473 We identified the *ZmUVR8* gene from *Zea mays* (*Zm*UVR8) using multiple sequence
474 comparison analysis. *ZmUVR8* gene expression is modulated by UV-B. The *Zm*UVR8
475 protein is highly conserved and has proven to be a functional homolog of the *Arabidopsis*
476 UV-B receptor *At*UVR8.

477
478
479
480
481
482
483
484
485
486
487
488
489
490
491
492
493

Supplementary figures

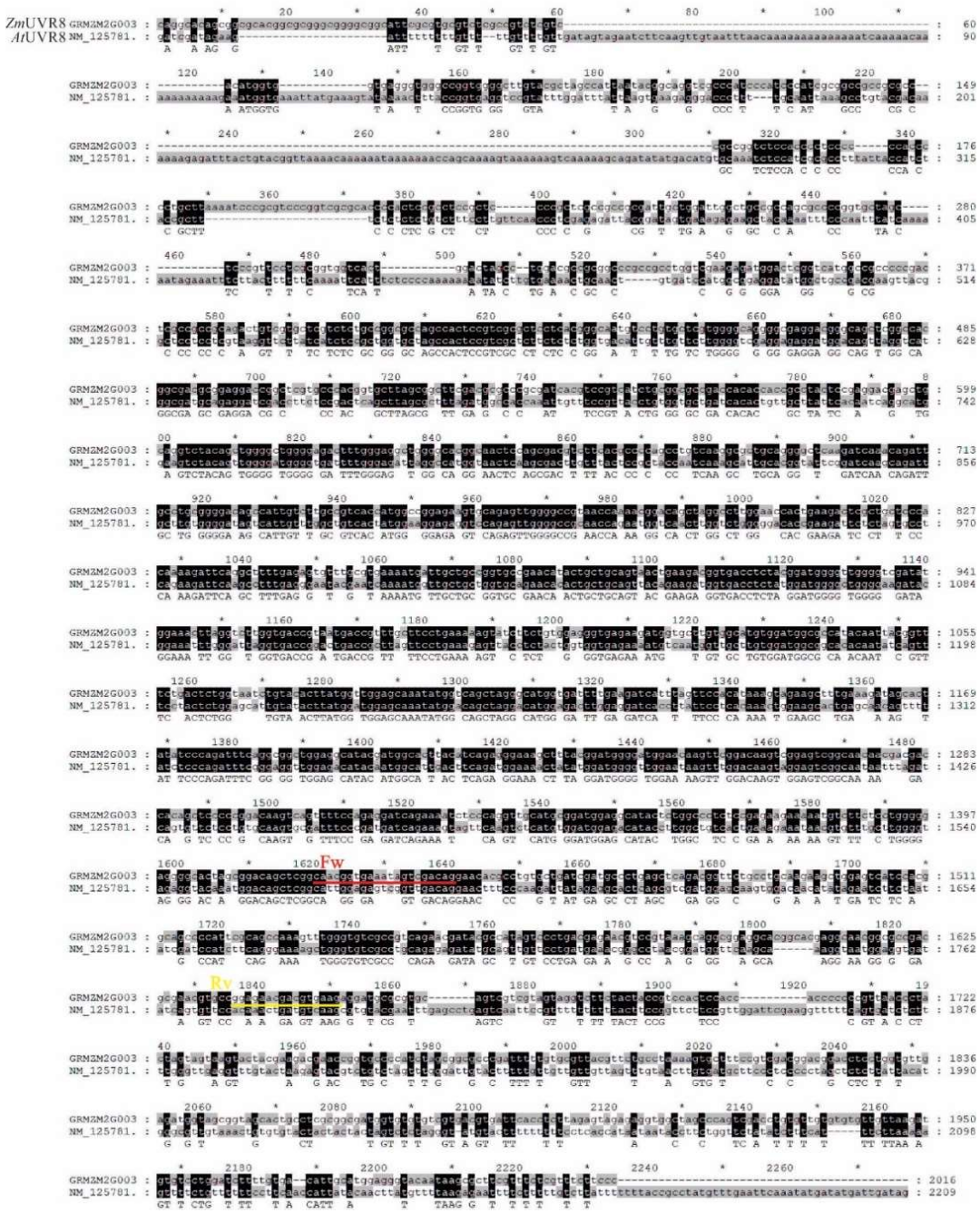

Fig. S1 Sequence alignment of *At*UVR8 and *Zm*UVR8 transcripts. UVR8 transcript sequences from maize (GRMZMG003565_T03) and *Arabidopsis* (NM_125781.4) were aligned using MAFFT software (http://mafft.cbrc.jp/alignment/server/) and edited with GeneDoc (Nicholas and Nicholas 1997). Forward (Fw) and reverse (Rv) *Zm*UVR8 primers used for quantitative RT- PCR are shown in red and yellow respectively. Conserved residues common to both sequences are shadowed in black and less identity is shown in gray scale. Capital letter indicates 100% of homology whereas lowercase indicates minor identity.

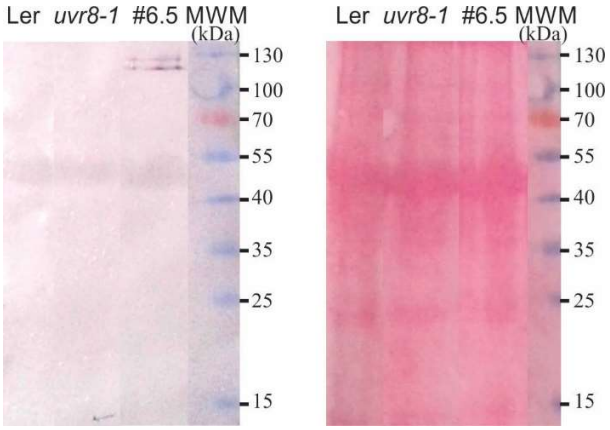

Fig. S2 *Zm*UVR8 detection by immunoblot. Non- boiled total protein extracts from Ler, *uvr8-1* and #6.5 transgenic line were separated on 12%SDS-PAGE and immunoblot was probed with anti-GFP antibody (left panel). Ponceau staining is shown as loading control (right panel). MWM: molecular weight markers.

Author Contributions

MF conducted experiments, interpreted data, drew figures, and collaborated in writing the manuscript. RC conceived the project and wrote the paper. LL supervised and improved the manuscript.

References

Brosché M, Strid A (2003) Molecular events following perception of ultraviolet-B radiation by plants. Physiol Plant 117:1-10

Brown BA, Cloix C, Jiang GH, Kaiserli E, Herzyk P, Kliebenstein DJ, Jenkins GI (2005) A UV-B-specific signaling component orchestrates plant UV protection. Proc Natl Acad Sci U S A 102:18225-18230 doi:0507187102 [pii] 10.1073/pnas.0507187102

Casati P, Campi M, Morrow DJ, Fernandes JF, Walbot V (2011a) Transcriptomic, proteomic and metabolomic analysis of UV-B signaling in maize. BMC Genomics 12:321 doi:1471-2164-12-321 [pii] 10.1186/1471-2164-12-321

Casati P, Morrow DJ, Fernandes JF, Walbot V (2011b) Rapid Maize Leaf and Immature Ear Responses to UV-B Radiation. Front Plant Sci 2:33 doi:10.3389/fpls.2011.00033

Casati P, Walbot V (2004) Rapid transcriptome responses of maize (Zea mays) to UV-B in irradiated and shielded tissues. Genome Biol 5:R16 doi:10.1186/gb-2004-5-3-r16 gb-2004-5-3-r16 [pii]

535 Cloix C et al. (2012) C-terminal region of the UV-B photoreceptor UVR8 initiates signaling through
536 interaction with the COP1 protein. Proc Natl Acad Sci U S A 109:16366-16370
537 doi:1210898109 [pii] 10.1073/pnas.1210898109
538 Clough SJ, Bent AF (1998) Floral dip: a simplified method for *Agrobacterium*-mediated
539 transformation of *Arabidopsis thaliana*. Plant J 16:735-743
540 Cnossen I, Sanz-Forcada J, Favata F, Witasse O, Zegers T, Arnold NF (2007) Habitat of early life: Solar
541 X-ray and UV radiation at Earth's surface 4–3.5 billion years ago. Geophys Res Lett 112:E2
542 Christie JM et al. (2012) Plant UVR8 photoreceptor senses UV-B by tryptophan-mediated disruption
543 of cross-dimer salt bridges. Science 335:1492-1496 doi:science.1218091 [pii]
544 10.1126/science.1218091
545 Favory JJ et al. (2009) Interaction of COP1 and UVR8 regulates UV-B-induced photomorphogenesis
546 and stress acclimation in *Arabidopsis*. EMBO J 28:591-601 doi:emboj20094 [pii]
547 10.1038/emboj.2009.4
548 Fernandez MB, Tossi V, Lamattina L, Cassia R (2016) A Comprehensive Phylogeny Reveals Functional
549 Conservation of the UV-B Photoreceptor UVR8 from Green Algae to Higher. Plants Front
550 Plant Sci 7:1698 doi:10.3389/fpls.2016.01698
551 Frohnmeyer H, Staiger D (2003) Ultraviolet-B radiation-mediated responses in plants. Balancing
552 damage and protection. Plant Physiol 133:1420-1428 doi:10.1104/pp.103.030049
553 133/4/1420 [pii]
554 Gao W, Zheng Y, Slusser JR, Heisler GM, Grant RH, Xu J, He D (2004) Effects of supplementary
555 ultraviolet-B irradiance on maize yield and qualities: a field experiment. Photochem
556 Photobiol 80:127-131 doi:10.1562/2004-05-03-RA-156.1
557 2004-05-03-RA-156 [pii]
558 Han X, Chang X, Zhang Z, Chen H, He H, Zhong B, Deng XW (2019) Origin and Evolution of Core
559 Components Responsible for Monitoring Light Environment Changes during Plant
560 Terrestrialization. Mol Plant 12:847-862 doi:S1674-2052(19)30135-2 [pii]
561 10.1016/j.molp.2019.04.006
562 Heijde M, Ulm R (2012) UV-B photoreceptor-mediated signalling in plants Trends Plant Sci 17:230-
563 237 doi:S1360-1385(12)00008-8 [pii] 10.1016/j.tplants.2012.01.007
564 Heilmann M, Jenkins GI (2013) Rapid reversion from monomer to dimer regenerates the ultraviolet-
565 B photoreceptor UV RESISTANCE LOCUS8 in intact *Arabidopsis* plants. Plant Physiol 161:547-
566 555 doi:pp.112.206805 [pii]
567 10.1104/pp.112.206805
568 Huang X, Yang P, Ouyang X, Chen L, Deng XW (2014) Photoactivated UVR8-COP1 module determines
569 photomorphogenic UV-B signaling output in *Arabidopsis.* PLoS Genet 10:e1004218
570 doi:10.1371/journal.pgen.1004218 PGENETICS-D-13-02962 [pii]
571 Jenkins GI (2014) The UV-B photoreceptor UVR8: from structure to physiology Plant Cell 26:21-37
572 doi:tpc.113.119446 [pii] 10.1105/tpc.113.119446
573 Jordan BR (1996) The effects of ultraviolet-B radiation on plants: a molecular perspective. Advances
574 in Botany 22:98-138
575 Kaiserli E, Jenkins GI (2007) UV-B promotes rapid nuclear translocation of the *Arabidopsis* UV-B
576 specific signaling component UVR8 and activates its function in the nucleus. Plant Cell
577 19:2662-2673 doi:tpc.107.053330 [pii] 10.1105/tpc.107.053330
578 Karimi M, Inze D, Depicker A (2002) GATEWAY vectors for *Agrobacterium*-mediated plant
579 transformation. Trends Plant Sci 7:193-195 doi:S1360-1385(02)02251-3 [pii]
580 Khudyakova AY et al. (2019) Impact of UV-B radiation on the photosystem II activity, pro-
581 /antioxidant balance and expression of light-activated genes in *Arabidopsis thaliana* hy4

582 mutants grown under light of different spectral composition. J Photochem Photobiol B
583 194:14-20 doi:S1011-1344(18)31461-1 [pii] 10.1016/j.jphotobiol.2019.02.003
584 Kim BC, Tennessen DJ, Last RL (1998) UV-B-induced photomorphogenesis in *Arabidopsis thaliana.*
585 Plant J 15:667-674
586 Kliebenstein DJ, Lim JE, Landry LG, Last RL (2002) *Arabidopsis* UVR8 regulates ultraviolet-B signal
587 transduction and tolerance and contains sequence similarity to human regulator of
588 chromatin condensation 1. Plant Physiol 130:234-243 doi:10.1104/pp.005041
589 Koncz C, Schell J (1986) The promoter of TL-DNA gene 5 controls the tissue- specific expression of
590 chimaeric gene carried by a novel type of *Agrobacterium* binary vector. Mol gen genet
591 204:383-396
592 Kondou Y et al. (2019) Physiological function of photoreceptor UVR8 in UV-B tolerance in the
593 liverwort *Marchantia polymorpha*. Planta 249:1349-1364 doi:10.1007/s00425-019-03090-
594 w10.1007/s00425-019-03090-w [pii]
595 Li H et al. (2018a) Tomato UV-B receptor SlUVR8 mediates plant acclimation to UV-B radiation and
596 enhances fruit chloroplast development via regulating SlGLK2. Sci Rep 8:6097
597 doi:10.1038/s41598-018-24309-y 10.1038/s41598-018-24309-y [pii]
598 Li X et al. (2018b) Molecular cloning and functional analysis of a UV-B photoreceptor gene, BpUVR8
599 (UV Resistance Locus 8), from birch and its role in ABA response. Plant Sci 274:294-308
600 doi:S0168-9452(17)31104-4 [pii]
601 10.1016/j.plantsci.2018.06.006
602 Liang T et al. (2018) UVR8 Interacts with BES1 and BIM1 to Regulate Transcription and
603 Photomorphogenesis in *Arabidopsis.* Dev Cell 44:512-523 e515 doi:S1534-5807(17)31079-1
604 [pii] 10.1016/j.devcel.2017.12.028
605 Liu L, Gregan S, Winefield C, Jordan B (2014) From UVR8 to flavonol synthase: UV-B-induced gene
606 expression in *Sauvignon* blanc grape berry. Plant Cell Environ 38:905-919
607 doi:10.1111/pce.12349
608 Llewellyn CA, Airs RL (2010) Distribution and abundance of MAAs in 33 species of microalgae across
609 13 classes. Mar Drugs 8:1273-1291 doi:10.3390/md8041273
610 Mao K, Wang L, Li YY, Wu R (2015) Molecular Cloning and Functional Analysis of UV RESISTANCE
611 LOCUS 8 (PeUVR8) from *Populus euphratica*. PLoS One 10:e0132390
612 doi:10.1371/journal.pone.0132390 PONE-D-15-04341 [pii]
613 Nicholas KB, Nicholas HBJ (1997) GeneDoc: a tool for editing and annotating multiple sequence
614 alignments.
615 O'Hara A, Jenkins GI (2012) In vivo function of tryptophans in the *Arabidopsis* UV-B photoreceptor
616 UVR8 Plant Cell 24:3755-3766 doi:tpc.112.101451 [pii] 10.1105/tpc.112.101451
617 Pearson WR (2014) An introduction to sequence similarity ("homology") searching. Curr Protoc
618 Bioinformatics Chapter 3:Unit3 1 doi:10.1002/0471250953.bi0301s42
619 Rajhi I et al. (2011) Identification of genes expressed in maize root cortical cells during lysigenous
620 aerenchyma formation using laser microdissection and microarray analyses. New Phytol
621 190:351-368 doi:10.1111/j.1469-8137.2010.03535.x
622 Rastogi RP, Incharoensakdi A (2013) UV radiation-induced accumulation of photoprotective
623 compounds in the green alga Tetraspora sp. CU2551. Plant Physiol Biochem 70:7-13
624 doi:S0981-9428(13)00159-9 [pii] 10.1016/j.plaphy.2013.04.021
625 Ren H et al. (2019) Two E3 ligases antagonistically regulate the UV-B response in *Arabidopsis.* Proc
626 Natl Acad Sci U S A doi:1816268116 [pii] 10.1073/pnas.1816268116
627 Rizzini L et al. (2011) Perception of UV-B by the *Arabidopsis* UVR8 protein Science 332:103-106
628 doi:332/6025/103 [pii] 10.1126/science.1200660

Rozema J et al. (2002) The role of UV-B radiation in aquatic and terrestrial ecosystems--an experimental and functional analysis of the evolution of UV-absorbing compounds. J Photochem Photobiol B 66:2-12 doi:S101113440100269X [pii]

Ruijter JM, Ramakers C, Hoogaars WM, Karlen Y, Bakker O, van den Hoff MJ, Moorman AF (2009) Amplification efficiency: linking baseline and bias in the analysis of quantitative PCR data. Nucleic Acids Res 37:e45 doi:gkp045 [pii] 10.1093/nar/gkp045

Sharma A, Sharma B, Hayes S, Kerner K, Hoecker U, Jenkins GI, Franklin KA (2019) UVR8 disrupts stabilisation of PIF5 by COP1 to inhibit plant stem elongation in sunlight. Nat Commun 10:4417 doi:10.1038/s41467-019-12369-1 10.1038/s41467-019-12369-1 [pii]

Soriano G, Cloix C, Heilmann M, Nunez-Olivera E, Martinez-Abaigar J, Jenkins GI (2018) Evolutionary conservation of structure and function of the UVR8 photoreceptor from the liverwort *Marchantia polymorpha* and the moss *Physcomitrella* patens. New Phytol 217:151-162 doi:10.1111/nph.14767

Strable J, Scanlon MJ (2009) Maize (Zea mays): a model organism for basic and applied research in plant biology. Cold Spring Harb Protoc 2009:pdb emo132 doi:2009/10/pdb.emo132 [pii] 10.1101/pdb.emo132

Sun K, Zhu Z (2018) Illuminating the Nucleus: UVR8 Interacts with More. Trends Plant Sci 23:279-281 doi:S1360-1385(18)30044-X [pii] 10.1016/j.tplants.2018.03.002

Tavridou E, Pireyre M, Ulm R (2019) Degradation of the transcription factors PIF4 and PIF5 under UV-B promotes UVR8-mediated inhibition of hypocotyl growth in *Arabidopsis.* Plant J doi:10.1111/tpj.14556

Tilbrook K, Arongaus AB, Binkert M, Heijde M, Yin R, Ulm R (2013) The UVR8 UV-B Photoreceptor: Perception, Signaling and Response Arabidopsis Book 11:e0164 doi:10.1199/tab.0164

Tilbrook K et al. (2016) UV-B perception and acclimation in *Chlamydomonas reinhardtii*. Plant Cell doi:tpc.15.00287 [pii] 10.1105/tpc.15.00287

Ulm R, Jenkins GI (2015) Q&A: How do plants sense and respond to UV-B radiation? BMC Biol 13:45 doi:10.1186/s12915-015-0156-y [pii]

Wu D et al. (2012) Structural basis of ultraviolet-B perception by UVR8. Nature 484:214-219 doi:nature10931 [pii] 10.1038/nature10931

Wu Q, Su N, Zhang X, Liu Y, Cui J, Liang Y (2016) Hydrogen peroxide, nitric oxide and UV RESISTANCE LOCUS8 interact to mediate UV-B-induced anthocyanin biosynthesis in radish sprouts. Sci Rep 6:29164 doi:srep29164 [pii] 10.1038/srep29164

Yang X, Montano S, Ren Z (2016) How does photoreceptor UVR8 perceive a UV- B signal? Photochem Photobiol 91:993- 1003

Yang Y et al. (2018) UVR8 interacts with WRKY36 to regulate HY5 transcription and hypocotyl elongation in *Arabidopsis*. Nat Plants 4:98-107 doi:10.1038/s41477-017-0099-0 10.1038/s41477-017-0099-0 [pii]

Yin R (2017) Cooling Down Thermomorphogenesis by UV-B Signaling. Trends Plant Sci 22:447-449 doi:S1360-1385(17)30068-7 [pii] 10.1016/j.tplants.2017.04.003

Yin R, Skvortsova MY, Loubery S, Ulm R (2016) COP1 is required for UV-B-induced nuclear accumulation of the UVR8 photoreceptor Proc Natl Acad Sci U S A 113:E4415-4422 doi:1607074113 [pii] 10.1073/pnas.1607074113

Yonekura-Sakakibara K, Higashi Y, Nakabayashi R (2019) The Origin and Evolution of Plant Flavonoid Metabolism. Front Plant Sci 10:943 doi:10.3389/fpls.2019.00943

Zeng X et al. (2015) Dynamic Crystallography Reveals Early Signalling Events in Ultraviolet Photoreceptor UVR8. Nat Plants 1 doi:10.1038/nplants.2014.6

675 Zhao C, Mao K, You CX, Zhao XY, Wang SH, Li YY, Hao YJ (2016) Molecular cloning and functional
676 analysis of a UV-B photoreceptor gene, MdUVR8 (UV Resistance Locus 8), from apple. Plant
677 Sci 247:115-126 doi:S0168-9452(16)30037-1 [pii] 10.1016/j.plantsci.2016.03.006